On Incompressibility Constraint and Crack Direction in Soft Solids

P. Mythravaruni
Faculty of Civil and Environmental Engineering,
Technion—I.I.T.,
Haifa 32000, Israel
e-mail: varuni.mythra@gmail.com

K. Y. Volokh
Faculty of Civil and Environmental Engineering,
Technion—I.I.T.,
Haifa 32000, Israel
e-mail: cvolokh@technion.ac.il

Most soft materials resist volumetric changes much more than shape distortions. This experimental observation led to the introduction of the incompressibility constraint in the constitutive description of soft materials. The incompressibility constraint provides analytical solutions for problems which, otherwise, could be solved numerically only. However, in the present work, we show that the enforcement of the incompressibility constraint in the analysis of the failure of soft materials can lead to somewhat nonphysical results. We use hyperelasticity with energy limiters to describe the material failure, which starts via the violation of the condition of strong ellipticity. This mathematical condition physically means inability of the material to propagate superimposed waves because cracks nucleate perpendicular to the direction of a possible wave propagation. By enforcing the incompressibility constraint, we sort out longitudinal waves, and consequently, we can miss cracks perpendicular to longitudinal waves. In the present work, we show that such scenario, indeed, occurs in the problems of uniaxial tension and pure shear of natural rubber. We also find that the suppression of longitudinal waves via the incompressibility constraint does not affect the consideration of the material failure in equibiaxial tension and the practically relevant problem of the failure of rubber bearings under combined shear and compression.
[DOI: 10.1115/1.4044089]

1 Introduction

Soft materials usually resist volumetric changes much more than shape distortions. This fact led to the explicit introduction of the incompressibility constraint in the constitutive description of soft materials. In the past, the incompressibility constraint led to elegant analytical solutions to otherwise intractable problems of nonlinear elasticity. Rivlin (1915–2005) pioneered and mastered this analytical approach [1]. Nowadays, computational methods do not need the exact incompressibility constraint because it is a problem from the computational standpoint. Nevertheless, the incompressibility constraint might still be helpful when looking for analytical solutions. In the present work, we study the role and effect of the incompressibility constraint on the analysis of the onset of material failure in soft isotropic solids.

Conventional hyperelastic models describe the mechanical response of intact materials. Hence, these models should ensure material stability and the existence of the solution of static boundary value problems. Such restrictions are often provided by the constitutive laws obeying the conditions of polyconvexity (and coercivity), strong ellipticity, Baker–Ericksen inequalities, etc. However, these restrictions must be relaxed to describe the material failure where damage nucleates and localizes into cracks. Evidently, such failure processes are generally dynamic, and consequently, it is natural and even necessary that the solutions of the static boundary value problems should not exist for propagating cracks.

Few hyperelastic constitutive models developed in the past could capture failure behavior [2–6]. However, the onset of failure reported in these works was a result of the specific and, probably, accidental choice of the material models. A more systematic traditional approach to failure description is based on continuum damage mechanics (CDM), in which an internal damage variable is introduced to reduce material stiffness. The damage variable is defined by the evolution equation when the damage threshold conditions are met [7–16]. We note that CDM is very useful for a description of gradual material damage as in the case of the Mullins effect in rubber-like materials, for example. CDM can also be used to describe abrupt material failure. However, in the latter case, a much simpler approach was developed [17], in which a limiter—the average bond energy—was introduced in the strain energy function, providing bounds of the reachable stresses. The bounded stresses naturally and automatically describe the material failure.

In the present work, we use hyperelasticity with energy limiters to analyze the onset of material failure and the direction of its localization in isotropic soft solids with and without the incompressibility constraint. The effect of the incompressibility constraint on the inception of the material failure is studied by tracking the strong ellipticity condition for the superimposed longitudinal and transverse waves. The incompressibility constraint suppresses longitudinal waves. By relaxing this constraint, it is possible to take longitudinal waves into consideration. We do that for natural rubber in the states of uniaxial and equibiaxial tension and pure shear. In addition, we also study the failure of rubber bearings under combined compression and shear, which is valuable for the structural design of seismic isolation, for example, [18].

2 Theoretical Background

Equations of balance for linear and angular momenta in the reference configuration Ω_0 read

$$\rho_0\ddot{\mathbf{y}} = \mathrm{Div}\,\mathbf{P}, \quad \mathbf{P}\mathbf{F}^{\mathrm{T}} = \mathbf{F}\mathbf{P}^{\mathrm{T}} \tag{1}$$

where ρ_0 is the mass density; $\mathbf{y}$ is the current position of a material particle, which occupied position $\mathbf{x}$ in the reference configuration; the divergence operator is with respect to $\mathbf{x}$; $\mathbf{P}$ is the first Piola-Kirchhoff stress; $\mathbf{F} = \mathrm{Grad}\,\mathbf{y}$ is the deformation gradient; and the body force is ignored.

For a hyperelastic material, the stress is given by

$$\mathbf{P} = \partial\psi/\partial\mathbf{F} \tag{2}$$

where ψ is the density of the strain energy.

The incompressibility constraint is introduced as

$$J \equiv \det\mathbf{F} = 1 \tag{3}$$

and the constitutive law is modified accordingly as

$$\mathbf{P} = \partial\psi/\partial\mathbf{F} - \Pi\mathbf{F}^{-\mathrm{T}} \tag{4}$$

where Π is a Lagrange multiplier.

Contributed by the Applied Mechanics Division of ASME for publication in the Journal of Applied Mechanics. Manuscript received April 23, 2019; final manuscript received June 14, 2019; published online July 17, 2019. Assoc. Editor: Shaoxing Qu.

In introducing the strain energy, we should note that the number of physical particles in a representative volume of real materials is limited. Consequently, the bond energy of these particles is limited. Thus, the strain energy density on the macroscopic scale should also be limited. Obviously, a limited strain energy automatically provides a limited stress, which a material can sustain. The latter condition of the limited or bounded stress is a qualitative indicator of the material failure.

The limiter can be introduced in the strain energy in the form as follows, for example:

$$\psi(\mathbf{F}) = \psi_{\mathrm{f}} - \psi_{\mathrm{e}}(\mathbf{F}) \tag{5}$$

where

$$\psi_{\mathrm{e}}(\mathbf{F}) = \Phi m^{-1}\Gamma(m^{-1},\, W(\mathbf{F})^m \Phi^{-m}), \quad \psi_{\mathrm{f}} = \psi_{\mathrm{e}}(\mathbf{1}) \tag{6}$$

with the identity tensor $\mathbf{1}$ and

$$\Gamma(s,\, x) = \int_x^\infty t^{s-1} e^{-t}\, dt$$

is the upper incomplete gamma function.

Here, we designated failure energy by ψ_{f} and elastic energy by $\psi_{\mathrm{e}}(\mathbf{F})$. The stored energy without failure is designated by $W(\mathbf{F})$ while Φ is the energy limiter (average bond energy) and m is a material parameter.

We note that the present formulation is valid for the analysis of the onset of failure. If the failure localization and propagation are of interest, then a regularized formulation should be used as in Refs. [19,20], for example.

The corresponding incremental equations, assuming the current configuration Ω as the referential one, are obtained by superimposing small increments on all variables [21]. Designating the increments with tildes, we have for the incremental momenta balance

$$\rho\ddot{\tilde{\mathbf{y}}} = \operatorname{div}\tilde{\boldsymbol{\sigma}}, \quad \tilde{\boldsymbol{\sigma}} + \boldsymbol{\sigma}\tilde{\mathbf{L}}^{\mathrm{T}} = (\tilde{\boldsymbol{\sigma}} + \boldsymbol{\sigma}\tilde{\mathbf{L}}^{\mathrm{T}})^{\mathrm{T}} \tag{7}$$

where $\rho = J^{-1}\rho_0$, the divergence operator is with respect to $\mathbf{y}$, $\boldsymbol{\sigma} = J^{-1}\mathbf{P}\mathbf{F}^{\mathrm{T}}$ is the Cauchy stress, $\tilde{\mathbf{L}} = \tilde{\mathbf{F}}\mathbf{F}^{-1}$, and $\tilde{\mathbf{F}} = \operatorname{Grad}\tilde{\mathbf{y}}$.

The incremental Cauchy stress is defined by the incremental constitutive law

$$\tilde{\boldsymbol{\sigma}} = \mathbb{A} : \tilde{\mathbf{L}} \tag{8}$$

and under the incremental incompressibility constraint

$$\operatorname{tr}\tilde{\mathbf{L}} = 0 \tag{9}$$

we have

$$\tilde{\boldsymbol{\sigma}} = \mathbb{A} : \tilde{\mathbf{L}} + \Pi\tilde{\mathbf{L}}^{\mathrm{T}} - \tilde{\Pi}\mathbf{1} \tag{10}$$

where the elasticity tensor $\mathbb{A}$ has the following Cartesian components

$$A_{ijkl} = J^{-1}F_{js}F_{lm}\frac{\partial^2\psi}{\partial F_{is}\partial F_{km}} \tag{11}$$

In the general compressible case, we choose strain energy $\psi(I_1, I_3)$ as a function of two invariants $I_1 = \operatorname{tr}\mathbf{B}$ and $I_3 = \det\mathbf{B}$, in which $\mathbf{B} = \mathbf{F}\mathbf{F}^{\mathrm{T}}$ is the left Cauchy-Green tensor; and we can directly calculate the components of the elasticity tensor as

$$\begin{aligned} JA_{ijkl} &= 2B_{jl}\delta_{ik}\psi_1 + 4B_{ji}B_{lk}\psi_{11} + 2(2\delta_{lk}\delta_{ji} - \delta_{li}\delta_{jk})I_3\psi_3 \\ &\quad + 4(B_{ji}\delta_{lk} + \delta_{ji}B_{lk})I_3\psi_{13} + 4I_3^2\delta_{ji}\delta_{lk}\psi_{33} \end{aligned} \tag{12}$$

where $\psi_k \equiv \partial\psi/\partial I_k$ and $\psi_{ks} \equiv \partial\psi_k/\partial I_s$.

A plane wave solution of the incremental equation (7) is assumed in the form

$$\tilde{\mathbf{y}} = \mathbf{r}g(\mathbf{s}\cdot\mathbf{y} - vt) \tag{13}$$

or under the incompressibility constraint as follows:

$$\tilde{\mathbf{y}} = \mathbf{r}g(\mathbf{s}\cdot\mathbf{y} - vt), \quad \tilde{\Pi} = \Upsilon g'(\mathbf{s}\cdot\mathbf{y} - vt) \tag{14}$$

where $\mathbf{r}$ and $\mathbf{s}$ are unit vectors in the direction of wave polarization and wave propagation, respectively; v is the speed of the wave; the prime denotes the derivative with respect to the argument of g; and Υ is the amplitude of the increment of the Lagrange multiplier.

Substituting the solution in the incremental equation (7), we get

$$\rho v^2\mathbf{r} = \boldsymbol{\Lambda}\mathbf{r} \tag{15}$$

or, under the incompressibility constraint,

$$\rho v^2\mathbf{r} = \boldsymbol{\Lambda}\mathbf{r} - \Upsilon\mathbf{s}, \quad \mathbf{r}\cdot\mathbf{s} = 0 \tag{16}$$

where $\boldsymbol{\Lambda}$ is the acoustic tensor with Cartesian components

$$\Lambda_{ik} = A_{ijkl}s_j s_l \tag{17}$$

In the present work, the strain energy ψ depends on I_1 and I_3 only, and the acoustic tensor is given by

$$\begin{aligned} J\boldsymbol{\Lambda} &= 2\psi_1(\mathbf{s}\cdot\mathbf{B}\mathbf{s})\mathbf{1} + 4\psi_{11}(\mathbf{B}\mathbf{s})\otimes(\mathbf{B}\mathbf{s}) + 2I_3(\psi_3 + 2I_3\psi_{33})\mathbf{s}\otimes\mathbf{s} \\ &\quad + 4I_3\psi_{13}(\mathbf{B}\mathbf{s}\otimes\mathbf{s} + \mathbf{s}\otimes\mathbf{B}\mathbf{s}) \end{aligned} \tag{18}$$

By taking the dot product of Eq. (15) or Eq. (16) with $\mathbf{r}$, we obtain the wave speed

$$\begin{aligned} J\rho v^2 &= J\mathbf{r}\cdot\boldsymbol{\Lambda}\mathbf{r} = 2\psi_1 a_1 + 4\psi_{11}a_2^2 + 2I_3(\psi_3 + 2I_3\psi_{33})a_3^2 \\ &\quad + 4I_3\psi_{13}a_2a_3 \end{aligned} \tag{19}$$

where

$$a_1 = \mathbf{s}\cdot\mathbf{B}\mathbf{s}, \quad a_2 = \mathbf{r}\cdot\mathbf{B}\mathbf{s}, \quad a_3 = \mathbf{r}\cdot\mathbf{s} \tag{20}$$

For the strain energy defined by Eq. (5), we further calculate

$$\begin{aligned} \psi_1 &= W_1 \exp[-W^m\Phi^{-m}] \\ \psi_3 &= W_3 \exp[-W^m\Phi^{-m}] \\ \psi_{13} &= (W_{13} - mW^{m-1}\Phi^{-m}W_1W_3)\exp[-W^m\Phi^{-m}] \\ \psi_{11} &= (W_{11} - mW^{m-1}\Phi^{-m}W_1^2)\exp[-W^m\Phi^{-m}] \\ \psi_{33} &= (W_{33} - mW^{m-1}\Phi^{-m}W_3^2)\exp[-W^m\Phi^{-m}] \end{aligned} \tag{21}$$

where $W_k \equiv \partial W/\partial I_k$ and $W_{ks} \equiv \partial W_k/\partial I_s$.

Substitution of Eq. (21) into Eq. (19) yields

$$J\rho v^2 = f_1 f_2 \tag{22}$$

where

$$\begin{aligned} f_1 &= 2W_1a_1 + 4(W_{11} - mW^{m-1}\Phi^{-m}W_1^2)a_2^2 \\ &\quad + 2I_3\{W_3 + 2I_3(W_{33} - mW^{m-1}\Phi^{-m}W_3^2)\}a_3^2 \\ &\quad + 4I_3(W_{13} - mW^{m-1}\Phi^{-m}W_1W_3)a_2a_3 \end{aligned} \tag{23}$$

and

$$f_2 = \exp[-W^m\Phi^{-m}] \tag{24}$$

The positive wave speed corresponds to the mathematical condition of the strong ellipticity of the incremental initial boundary value problem. Zero wave speed mathematically means violation of the strong ellipticity condition, and physically, it means inability of the material to propagate a wave in direction $\mathbf{s}$. The latter notion can also be interpreted as the onset of a crack perpendicular to $\mathbf{s}$. The reader is also referred to the pioneering works [22–25] for further background.

3 Uniaxial Tension, Pure Shear, and Equibiaxial Tension With and Without the Incompressibility Constraint

In this section, we determine the onset of failure localization in isotropic compressible and incompressible materials via the condition of the zero velocity of the superimposed wave.

The predeformation is given as follows:

$$y_1 = \lambda_1 x_1, \quad y_2 = \lambda_2 x_2, \quad y_3 = \lambda_3 x_3 \tag{25}$$

where λ_1, λ_2, and λ_3 are the principal axial stretches and $\lambda_3 = \lambda_1^{-1}\lambda_2^{-1}$ for incompressible materials.

The deformation gradient and the left Cauchy-Green tensors are then calculated as

$$\begin{aligned} \mathbf{F} &= \lambda_1 \mathbf{e}_1 \otimes \mathbf{e}_1 + \lambda_2 \mathbf{e}_2 \otimes \mathbf{e}_2 + \lambda_3 \mathbf{e}_3 \otimes \mathbf{e}_3 \\ \mathbf{B} &= \lambda_1^2 \mathbf{e}_1 \otimes \mathbf{e}_1 + \lambda_2^2 \mathbf{e}_2 \otimes \mathbf{e}_2 + \lambda_3^2 \mathbf{e}_3 \otimes \mathbf{e}_3 \end{aligned} \tag{26}$$

where $\mathbf{e}_1$, $\mathbf{e}_2$, and $\mathbf{e}_3$ are the Cartesian basis vectors.

Plane longitudinal wave (P-wave) is defined by the following direction and polarization vectors:

$$\mathbf{s} = \mathbf{r} = \cos\alpha \mathbf{e}_1 + \sin\alpha \mathbf{e}_2 \tag{27}$$

where α is the angle from x_1 in plane (x_1, x_2).

A plane transverse wave (S-wave) is defined by the mutually perpendicular direction and polarization vectors

$$\mathbf{s} = \cos\alpha \mathbf{e}_1 + \sin\alpha \mathbf{e}_2, \quad \mathbf{r} = -\sin\alpha \mathbf{e}_1 + \cos\alpha \mathbf{e}_2 \tag{28}$$

Then, we evaluate the following quantities for the P-wave

$$a_1 = a_2 = \lambda_1^2 \cos^2\alpha + \lambda_2^2 \sin^2\alpha, \quad a_3 = 1 \tag{29}$$

and for the S-wave

$$a_1 = \lambda_1^2 \cos^2\alpha + \lambda_2^2 \sin^2\alpha, \quad a_2 = (\lambda_2^2 - \lambda_1^2)\sin(2\alpha)/2, \quad a_3 = 0 \tag{30}$$

We use the Yeoh stored energy function for the intact material behavior

$$W = \sum_{i=1}^{3} c_i (I_3^{-1/3} I_1 - 3)^i + \frac{K}{4}(I_3 - 1 - \ln I_3) \tag{31}$$

with material constants given in Table 1 [26].

The bulk modulus K is fitted from the condition that the stress–stretch curves for slightly compressible and incompressible materials coincide.

The split conditions of the material failure are

$$f_1 = 0 \quad \text{or} \quad f_2 = 0 \tag{32}$$

We emphasize that the second condition, $f_2 = 0$, makes sense *numerically* because the exponential function $f_2 = \exp[-W^m \Phi^{-m}]$ approaches zero very fast.

For the compressible material, we note that principal stretch λ_3 is determined implicitly (and numerically) in terms of λ_1 and λ_2 from the condition $\sigma_3 = 0$. In the case of the incompressible material, $\lambda_3 = \lambda_1^{-1}\lambda_2^{-1}$ and Lagrange multiplier Π is determined from the condition $\sigma_3 = 0$. The principal stretches in the plane of the sample are related as $\lambda_2 = \lambda_1^n$, where n is the biaxiality ratio. For uniaxial tension in the x_1 direction, $n = -0.5$; for pure shear in the x_1 direction, $n = 0$; and for equibiaxial tension in the (x_1, x_2) plane, $n = 1$.

Table 1 Material constants for the model

c_1 (MPa)	c_2 (MPa)	c_3 (MPa)	Φ (MPa)	K (MPa)	m
0.298	0.014	0.00016	69.4	4000	50

In what follows, we find the critical stretches corresponding to the loss of the strong ellipticity. We analyze three cases.

(a) Longitudinal P-wave for slightly compressible material.
(b) Transverse S-wave for slightly compressible material.
(c) Transverse S-wave for incompressible material.

We found that the results for S-waves—cases (b) and (c)—were numerically close.

Figure 1 shows the dependence of λ_1 on α obeying the failure conditions (Eq. (32)) for the P-wave in slightly compressible materials. The lowest magnitude of λ_1 violating the strong ellipticity condition occurs for $\alpha = 0$ deg, which means that the failure localizes in direction x_2 and the crack appears in the direction perpendicular to the load. The latter conclusion is correct for the cases of pure shear and uniaxial tension. In the case of the equibiaxial tension, there is no preferred direction of the crack localization as expected.

Figure 2 shows the dependence of λ_1 on α obeying the failure conditions (Eq. (32)) for the S-wave in the slightly compressible and incompressible materials. The lowest critical magnitude of λ_1 occurs for $\alpha = 83$ deg which means that failure localizes at the

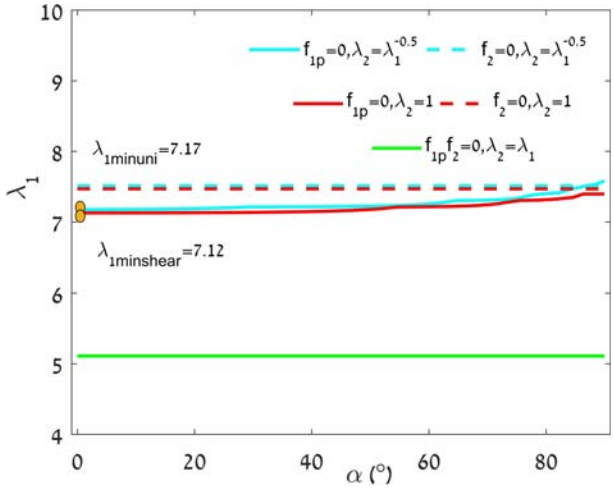

Fig. 1 P-wave: critical uniaxial stretch λ_1 versus α for different biaxiality ratios (−0.5, 0, and 1). Curves $f_{1p} = 0$ and $f_2 = 0$ are presented. The minimum amount of stretch indicates the material instability inception via the loss of strong ellipticity.

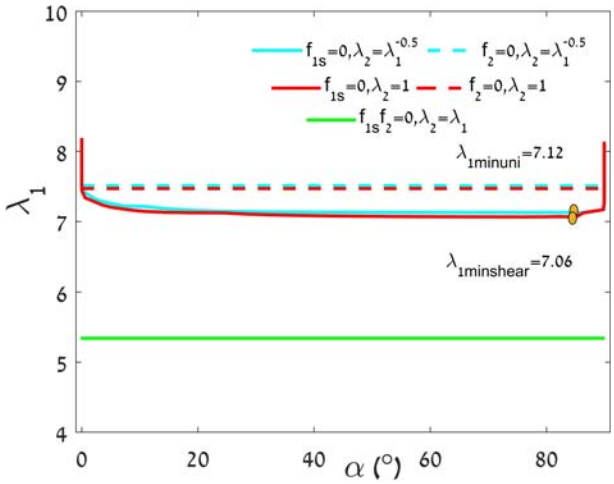

Fig. 2 S-wave: critical uniaxial stretch λ_1 versus α for different biaxiality ratios (−0.5, 0, and 1). Curves $f_{1s} = 0$ and $f_2 = 0$ are presented. The minimum amount of stretch indicates the material instability inception via the loss of strong ellipticity.

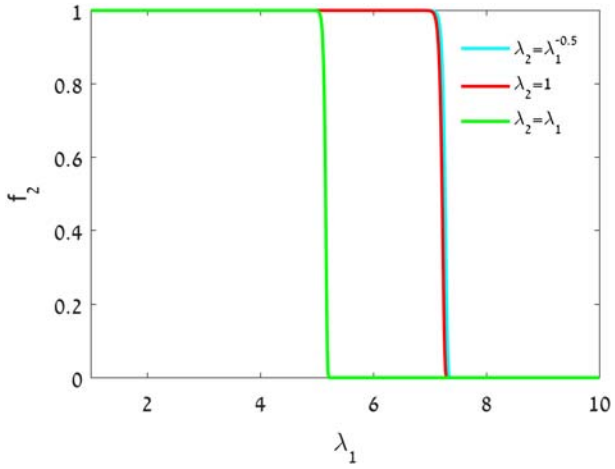

Fig. 3 Convergence of f_2 to zero for different biaxiality ratios (−0.5, 0, and 1)

angle of 7 deg in the first quadrant. Hence, the crack is not perpendicular to the direction of stretching in the cases of uniaxial tension and pure shear.

The exponentially varying function f_2 with the stretch λ_1 is shown graphically in Fig. 3. We emphasize that theoretically, the exponential function converges to zero at infinity. However, the "numerical infinity" is close and the convergence to it is fast.

Figure 4 shows the dependence of the Cauchy stress on the amount of stretch. The dark colored and light colored points denote the loss of strong ellipticity for S- and P-waves, respectively.

In summary, the cracks are correctly predicted by longitudinal waves but not by transverse waves. Thus, the incompressibility constraint, suppressing the longitudinal waves, leads to the appearance of nonphysical results concerning the direction of cracks.

Remark 1. We emphasize that it is not the superimposed wave which triggers fracture. We analyze only the possibility of the wave to propagate. In the presence of a crack, the wave cannot propagate whether it is transverse or longitudinal. We also note that our analysis is based on the assumption of the vanishing wave speed. In the case of nonvanishing wave speed, the analysis becomes more complicated [27], yet we do not need it. ■

Remark 2. Generally, condition $\det \mathbf{\Lambda} = 0$ can be used in analysis instead of $\mathbf{r} \cdot \mathbf{\Lambda r} = 0$. We used both conditions in the case of uniaxial tension, and they gave the same critical stretch (for P-wave).

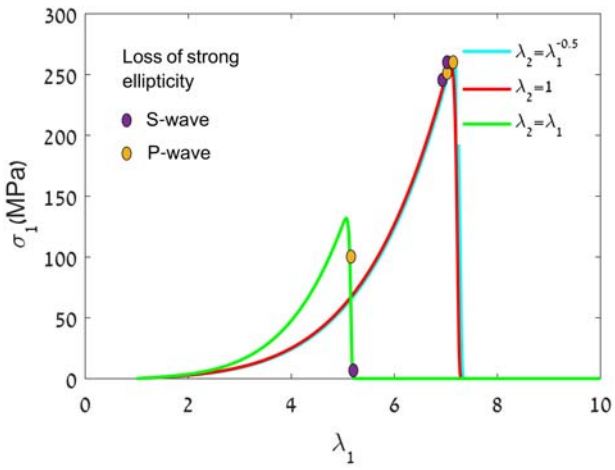

Fig. 4 Cauchy stress (MPa) versus stretch λ_1 in the x_1 direction for uniaxial tension, pure shear, and equibiaxial tension. The dark colored and light colored points denote the loss of strong ellipticity for S- and P-waves, respectively.

However, condition $\det \mathbf{\Lambda} = 0$ produced the second critical stretch (for P-wave), which was only half as large as the first one. The latter critical stretch is not physical and it contradicts experiments. We attribute the appearance of this "parasitic" solution to the formal mathematical condition $\det \mathbf{\Lambda} = 0$, which creates multiplicity of solutions without sorting out the physically meaningless ones. This probably happens because condition $\det \mathbf{\Lambda} = 0$ does not have a direct physical interpretation while condition $\mathbf{r} \cdot \mathbf{\Lambda r} = 0$ is a direct expression for the vanishing wave speed. The latter condition is evidently more physically appealing and mathematically restrictive, and therefore, it is preferred. ■

4 Combined Shear and Compression With and Without Incompressibility Constraint

In this section, we study the loss of the strong ellipticity for rubber bearings subjected to combined compression and shear. Such problem was considered in Ref. [28] for S-wave under the incompressibility constraint. Below, we examine the problem without the constraint for P-wave.

The deformation is of the form [29,30]

$$y_1 = \lambda_1 x_1 + \lambda_2 \gamma x_2, \quad y_2 = \lambda_2 x_2, \quad y_3 = \lambda_3 x_3 \tag{33}$$

where γ is the amount of shear.

Then, we have

$$\mathbf{F} = \lambda_1 \mathbf{e}_1 \otimes \mathbf{e}_1 + \lambda_2 \gamma \mathbf{e}_1 \otimes \mathbf{e}_2 + \lambda_2 \mathbf{e}_2 \otimes \mathbf{e}_2 + \lambda_3 \mathbf{e}_3 \otimes \mathbf{e}_3$$

$$\mathbf{B} = (\lambda_1^2 + \lambda_2^2 \gamma^2)\mathbf{e}_1 \otimes \mathbf{e}_1 + \lambda_2^2 \gamma \mathbf{e}_1 \otimes \mathbf{e}_2 + \lambda_2^2 \gamma \mathbf{e}_2 \otimes \mathbf{e}_1 + \lambda_2^2 \mathbf{e}_2 \otimes \mathbf{e}_2 + \lambda_3^2 \mathbf{e}_3 \otimes \mathbf{e}_3 \tag{34}$$

and for the longitudinal wave, we get

$$a_1 = a_2 = (\lambda_1^2 + \lambda_2^2 \gamma^2)\cos^2 \alpha + \gamma \lambda_2^2 \sin(2\alpha) + \lambda_2^2 \sin^2 \alpha, \quad a_3 = 1 \tag{35}$$

Material instability sets in when the P-wave speed is zero

$$J \rho v_p^2 = f_{1p} f_{2p} = 0 \tag{36}$$

We use the same constitutive model as in Sec. 3. Based on the results of the previous section concerning the use of the computational incompressibility condition, we approximately assume in computations: $\lambda_1 = \lambda_3 \cong \lambda^{-1/2}$ and $\lambda_2 \cong \lambda$.

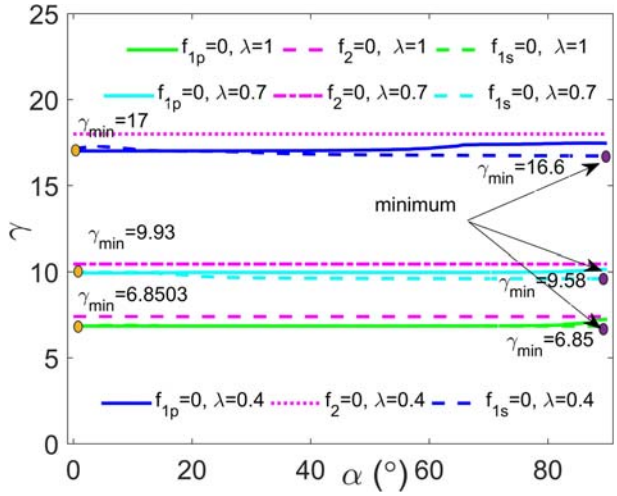

Fig. 5 Amount of shear versus the orientation of the superimposed wave. Curves $f_{1s} = 0$ and $f_2 = 0$ are presented for various values of compression for the S-wave analysis [28]. Curves $f_{1p} = 0$ and $f_2 = 0$ are presented for various values of compression for the P-wave analysis. The minimum amount of shear corresponds to the beginning of instability via the loss of strong ellipticity.

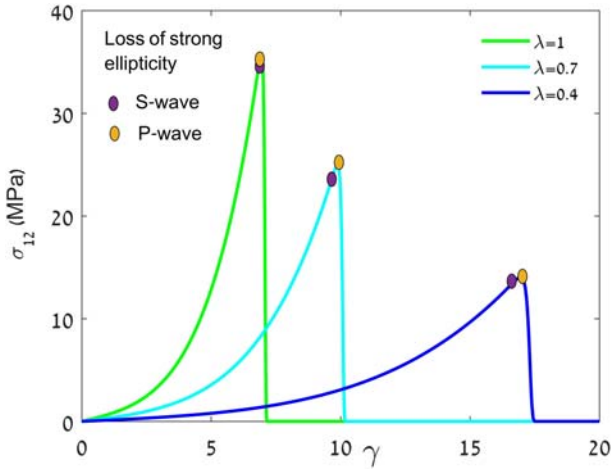

Fig. 6 Shear stress versus amount of shear. The dark colored and light colored points denote the loss of strong ellipticity for transverse and longitudinal waves, respectively.

We study the effect of compression on the onset of material instability for three values of the stretch: $\lambda_2 = 1, 0.7, 0.4$. The comparison between these results for the superimposed P-wave with the results for the superimposed S-wave [28] is given in Fig. 5.

Figure 5 shows that the lowest critical amount of shear is always obtained for $\alpha = 90$ deg, which means that failure localizes along x_1 and, consequently, the crack should appear in the horizontal direction in incompressible rubber bearings in accordance with the on-site observations [31]. At the same time, considering the P-wave, cracks might appear in the vertical direction, which was not observed experimentally previously.

Figure 6 shows the dependence of the Cauchy shear stress on the amount of stretch. The dark colored and light colored points denote the loss of strong ellipticity for S- and P-waves, respectively.

5 Conclusion

We used hyperelasticity with energy limiters to describe the material failure. We assumed that failure started via the violation of the condition of strong ellipticity, which physically meant inability of material to propagate superimposed waves. We found that the incompressibility constraint suppressed longitudinal waves and, consequently, prevented from the prediction of cracks, which were intuitively appealing and experimentally observed in uniaxial tension and pure shear. In addition to the tension problems, we considered the practically interesting problem of the failure of rubber bearings under combined shear and compression. We found that the prediction of the experimentally observed crack was not affected by the incompressibility constraint because it was related to the propagation of transverse wave.

We conclude that the incompressibility constraint can turn into a Trojan Horse in the analytical calculations. Its use should be careful and well designed.

Finally, we note that the recent experimental work [32] reported a counter-intuitive observation of cracks in the direction of tension in a silicone elastomer. The authors of the work attributed these "sideways" cracks to "microstructural anisotropy (in a nominally isotropic elastomer)." However, our results presented in Fig. 2 predict a possible onset of cracks leaning to the direction of tension.

Acknowledgment

Comments and discussion by Professor Michel Destrade are highly appreciated. The support from the Israel Science Foundation (ISF-198/15; Funder ID: 10.13039/501100003977) is gratefully acknowledged.

References

[1] Barenblatt, G. I., and Joseph, D. D., 1997, *Collected Papers of R. S. Rivlin*, Vols. 1–2, Springer, New York.
[2] Kurashige, M., 1981, "Instability of a Transversely Isotropic Elastic Slab Subjected to Axial Loads," J. Appl. Mech., **48**(2), pp. 351–356.
[3] Triantafyllidis, N., and Abeyaratne, R., 1983, "Instability of a Finitely Deformed Fiber-Reinforced Elastic Material," J. Appl. Mech., **50**(1), pp. 149–156.
[4] Danescu, A., 1991, "Bifurcation in the Traction Problem for a Transversely Isotropic Material," Math. Proc. Camb. Philos. Soc., **110**(2), pp. 385–394.
[5] Merodio, J., and Ogden, R. W., 2002, "Material Instabilities in Fiber-Reinforced Nonlinearly Elastic Solids Under Plane Deformation," Arch. Mech., **54**(5–6), pp. 525–552.
[6] Dorfmann, L., and Ogden, R. W., eds., 2015, Nonlinear Mechanics of Soft Fibrous Materials, Springer, Wien.
[7] Simo, J. C., 1987, "On a Fully Three-Dimensional Finite Strain Viscoelastic Damage Model: Formulation and Computational Aspects," Comput. Methods Appl. Mech. Eng., **60**(2), pp. 153–173.
[8] Govindjee, S., and Simo, J. C., 1991, "A Micro-Mechanically Based Continuum Damage Model of Carbon Black-Filled Rubbers Incorporating the Mullins Effect," J. Mech. Phys. Solids, **39**(1), pp. 87–112.
[9] Johnson, M. A., and Beatty, M. F., 1993, "A Constitutive Equation for the Mullins Effect in Stress Controlled in Uniaxial Extension Experiments," Contin. Mech. Thermodyn., **5**(4), pp. 301–318.
[10] Miehe, C., 1995, "Discontinuous and Continuous Damage Evolution in Ogden-Type Large-Strain Elastic Materials," Eur. J. Mech. A/Solids, **14**(5), pp. 697–720.
[11] De Souza Neto, E. A., Peric, D., and Owen, D. R. J., 1998, "Continuum Modeling and Numerical Simulation of Material Damage at Finite Strains," Arch. Comput. Methods Eng., **5**, pp. 311–384.
[12] Ogden, R. W., and Roxburgh, D. G., 1999, "A Pseudo-Elastic Model for the Mullins Effect in Filled Rubber," Proc. R. Soc. Lond. Ser. A, **455**, pp. 2861–2877.
[13] Menzel, A., and Steinmann, P., 2001, "A Theoretical and Computational Framework for Anisotropic Continuum Damage Mechanics at Large Strains," Int. J. Solids Struct., **38**(52), pp. 9505–9523.
[14] Guo, Z., and Sluys, L., 2006, "Computational Modeling of the Stress-Softening Phenomenon of Rubber Like Materials Under Cyclic Loading," Eur. J. Mech. A/Solids, **25**(6), pp. 877–896.
[15] De Tommasi, D., Puglisi, G., and Saccomandi, G., 2008, "Localized Vs Diffuse Damage in Amorphous Materials," Phys. Rev. Lett., **100**, 085502.
[16] Dal, H., and Kaliske, M., 2009, "A Micro-Continuum-Mechanical Material Model for Failure of Rubberlike Materials: Application to Ageing-Induced Fracturing," J. Mech. Phys. Solids, **57**(8), pp. 1340–1356.
[17] Volokh, K. Y., 2013, "Review of the Energy Limiters Approach to Modeling Failure of Rubber," Rubber Chem. Technol., **86**(3), pp. 470–487.
[18] Gent, A. N., 2001, *Engineering With Rubber*, 2nd ed., Hanser, Munich.
[19] Volokh, K. Y., 2017, "Fracture as a Material Sink," Mater. Theory, **1**(1), 3.
[20] Faye, A., Lev, Y., and Volokh, K. Y., 2019, "The Effect of Local Inertia Around the Crack Tip in Dynamic Fracture of Soft Materials," Mech. Soft Mater., **1**(1), 4.
[21] Volokh, K. Y., 2016, *Mechanics of Soft Materials*, Springer, Singapore.
[22] Hadamard, J., 1903, *Lecons sur la Propagation des Ondes et les Equations de L'Hydrodynamique*, Librairie Scientifique A. Hermann, Paris.
[23] Hill, R., 1962, "Acceleration Waves in Solids," J. Mech. Phys. Solids, **10**(1), pp. 1–16.
[24] Mandel, J., 1966, "Conditions de stabi1ite et postulat de Drucker," *Rheology and Soil Mechanics*, J. Kravtchenko and P. M. Sirieys, eds., Springer-Verlag, New York, pp. 58–68.
[25] Rice, J. R., 1976, "The Localization of Plastic Deformation," Theoretical and Applied Mechanics (Proceedings of the 14th International Congress on Theoretical and Applied Mechanics, Delft, 1976, W. T. Koiter, ed.), Vol. 1, North-Holland Publishing Co., Amsterdam, pp. 207–220.
[26] Volokh, K. Y., 2010, "On Modeling Failure of Rubberlike Materials," Mech. Res. Commun., **37**(8), pp. 684–689.
[27] Ting, T. C. T., 2006, "Longitudinal and Transverse Waves in Anisotropic Elastic Materials," Acta Mech., **185**(3–4), pp. 147–164.
[28] Mythravaruni, P., and Volokh, K. Y., 2018, "Failure of Rubber Bearings Under Combined Shear and Compression," ASME J. Appl. Mech., **85**(7), 074503.
[29] Rajagopal, K. R., and Wineman, A. S., 1987, "New Universal Relations for Nonlinear Isotropic Elastic Materials," J. Elast., **17**(1), pp. 75–83.
[30] Mihai, L. A., Budday, S., Holzapfel, G. A., Kuhl, E., and Goriely, A., 2017, "A Family of Hyperelastic Models for Human Brain Tissue," J. Mech. Phys. Solids, **106**, pp. 60–79.
[31] Takahashi, Y., 2012, "Damage of Rubber Bearings and Dumpers of Bridges in 2011 Great East Japan Earthquake," Proceedings of the International Symposium on Engineering, Lessons Learned From the 2011 Great East Japan Earthquake, Tokyo, Japan, Mar. 1–4.
[32] Lee, S., and Pharr, M., 2019, "Sideways and Stable Crack Propagation in a Silicone Elastomer," Proc. Natl. Acad. Sci. U.S.A., **116**(19), pp. 9251–9256.